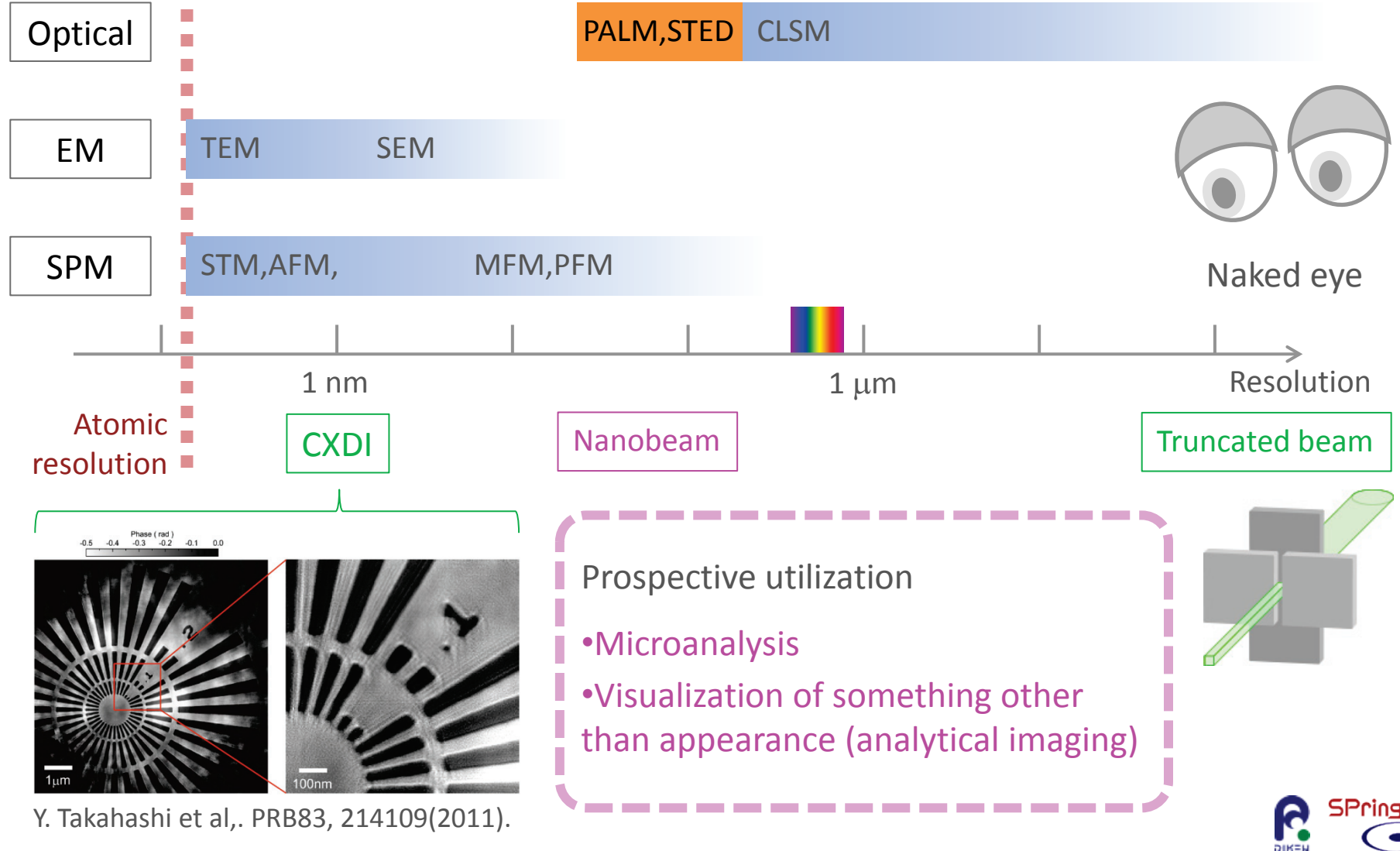


顕微計測が実現する マルチスケール構造物性研究



理研放射光科学総合研究センター 大隅寛幸

Microscopy



Outline

1. Microanalysis
 - X-ray focusing optics at BL19LXU/SPring-8
 - Operand XRD measurement on an EDLT device
2. Visualization of domain structures
 - Polarized X-ray diffractometry
 - Chirality domain structure of CsCuCl_3
 - Antiferromagnetic domain structure of $\text{Cd}_2\text{Os}_2\text{O}_7$
3. Expectations for the next generation light source
 - Evaluation of L/S by NRXMS: Sr_2IrO_4
 - Discrimination of spin chirality by NRXMS: DyMnO_3
 - Improvement in the photon flux density

Collaborators

SPring-8

T. Arima (*RSC / Univ. of Tokyo*)

S. Tardif (*RSC*)

T. Komesu (*RSC*)

N. Kawamura (*JASRI*)

H. Ohashi (*JASRI*)

CsCuCl₃

Y. Kousaka (*Aoyama-Gakuin Univ.*)

Y. Nakao (*Aoyama-Gakuin Univ.*)

Cd₂Os₂O₇

Z. Hiroi (*Univ. of Tokyo*)

N. Torimoto (*Kwansei-Gakuin Univ.*)

Sr₂IrO₄

B. J. Kim (*Univ. of Tokyo*)

S. Fujiyama (*RIKEN*)

DyMnO₃

H. Sagayama (*Tohoku Univ.*)

N. Abe (*Tohoku Univ.*)

K. Taniguchi (*Tohoku Univ.*)

M. Takata (*RIKEN SPring-8 Center*)

S. Takeshita (*RSC*)

M. Suzuki (*JASRI*)

H. Yumoto (*JASRI*)

T. Koyama (*JASRI*)

J. Akimitsu (*Aoyama-Gakuin Univ.*)

T. Yokobori (*Aoyama-Gakuin Univ.*)

J. Yamaura (*Tokyo tech*)

S. Kawase (*Kwansei-Gakuin Univ.*)

H. Takagi (*Univ. of Tokyo*)

D. Hirai (*Univ. of Tokyo*)

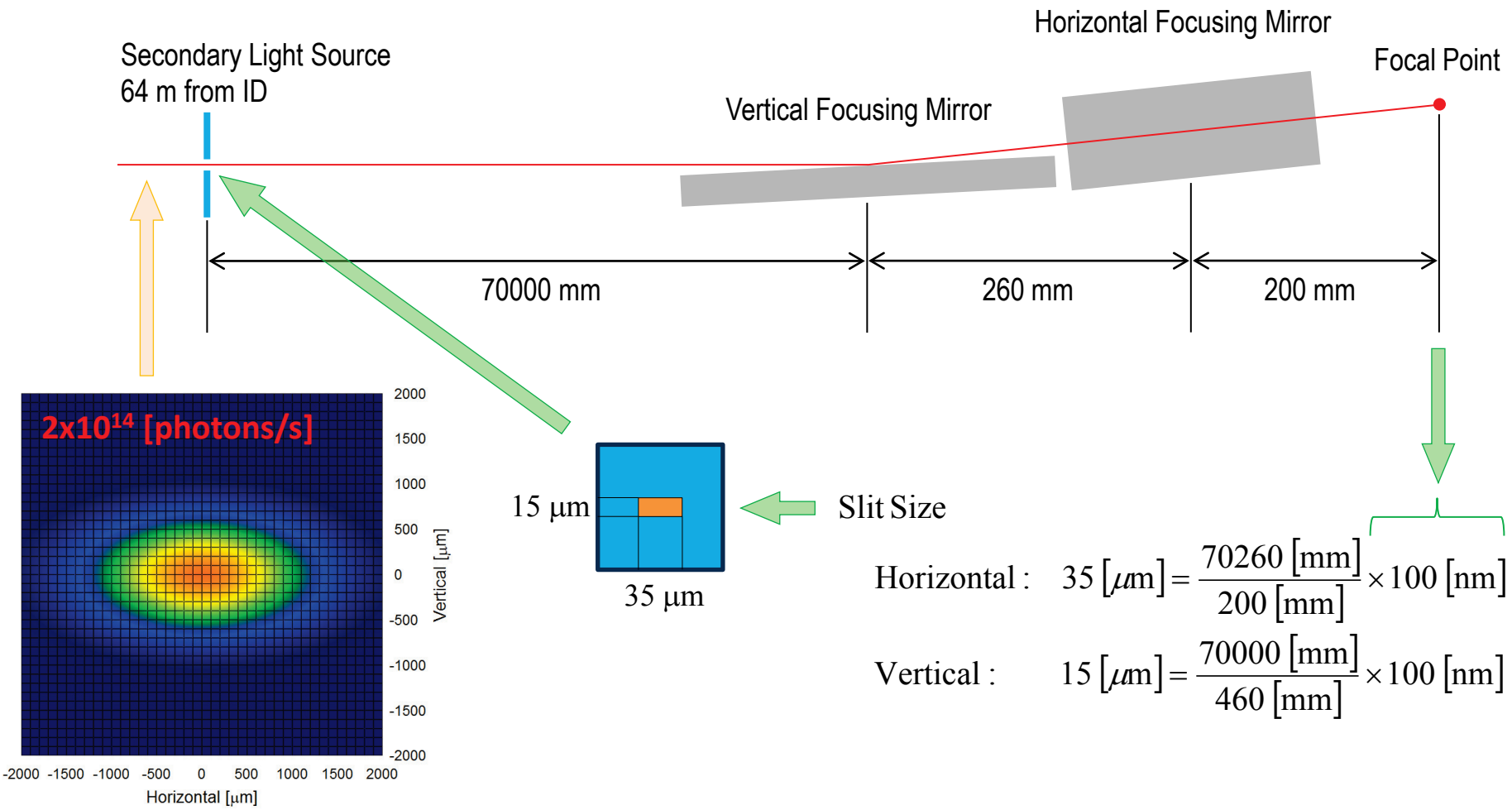
Y. Tokura (*Univ. of Tokyo*)

D. Okuyama (*RIKEN ASI*)

Y. Yamasaki (*Univ. of Tokyo*)

X-ray focusing optics in BL19LXU/SPring-8

BL19LXU/SPring-8

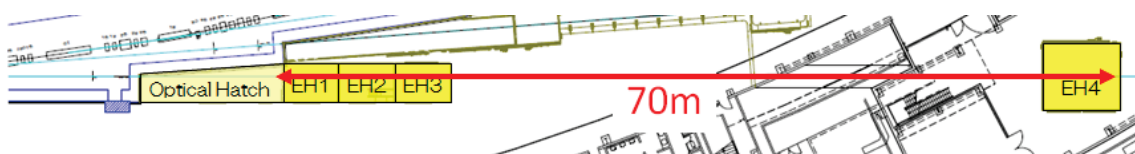


X-ray nanobeam available at BL19LXU/SPring-8

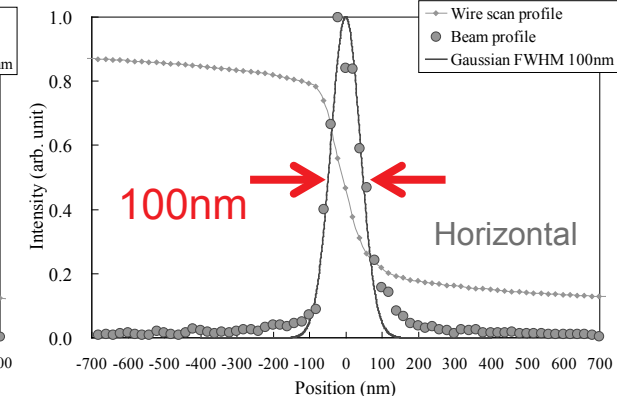
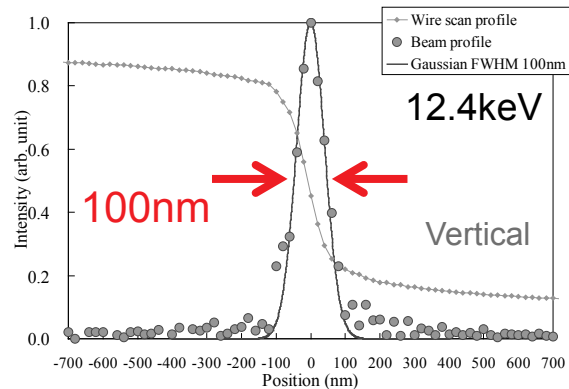
BL19LXU/SPring-8



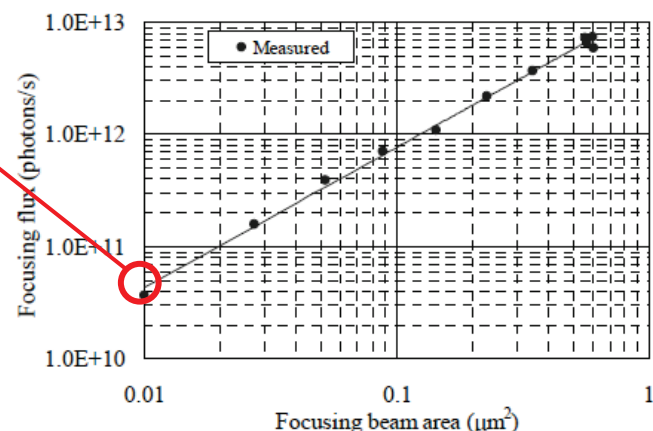
KB mirror optics



Focusing intensity profile and photon flux

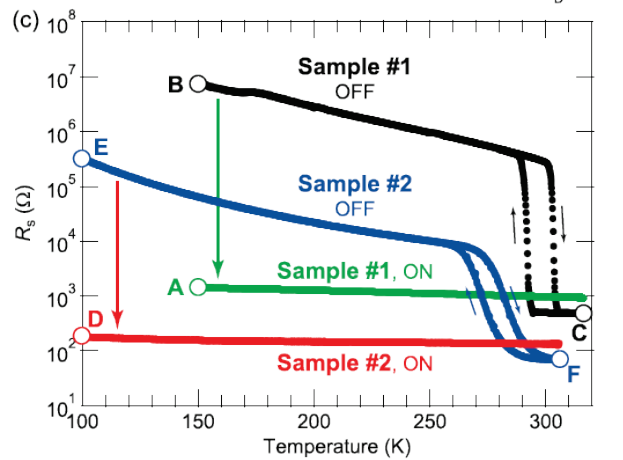
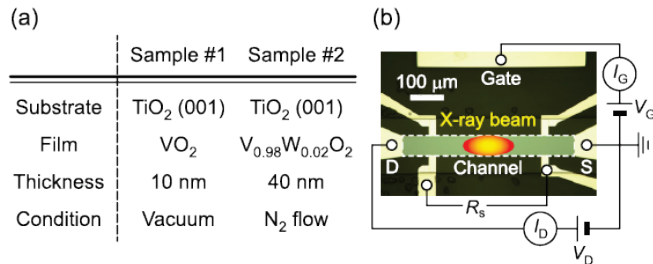


3.7×10^{10} photons/s
@ $100 \times 100 \text{ nm}^2$

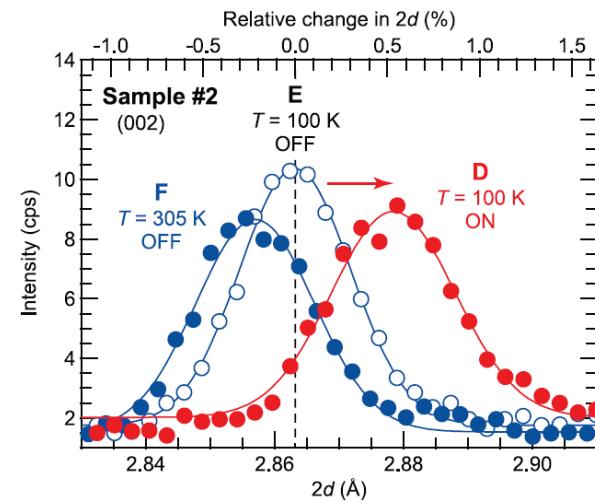
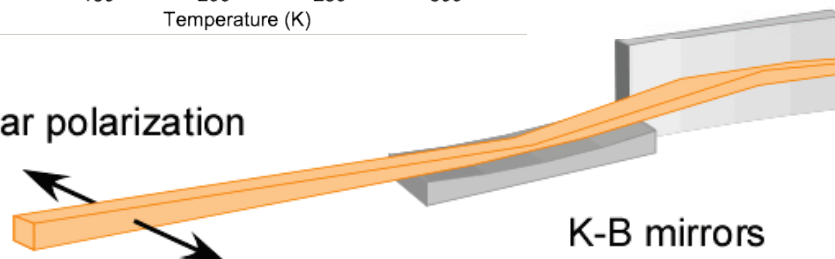


Operand XRD measurement on an EDLT device

VO₂ – electric-double layer transistor

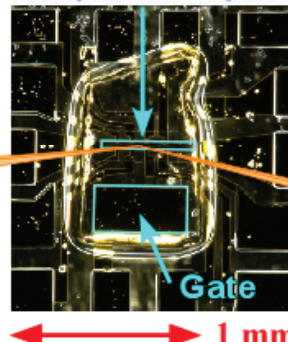


Linear polarization



XRD patterns of the 002 reflection

Channel
60 μm x 500 μm



Detector

Outline

1. Microanalysis

- X-ray focusing optics at BL19LXU/SPring-8
- Operand XRD measurement on an EDLT device

2. Visualization of domain structures

- Polarized X-ray diffractometry
- Chirality domain structure of CsCuCl_3
- Antiferromagnetic domain structure of $\text{Cd}_2\text{Os}_2\text{O}_7$

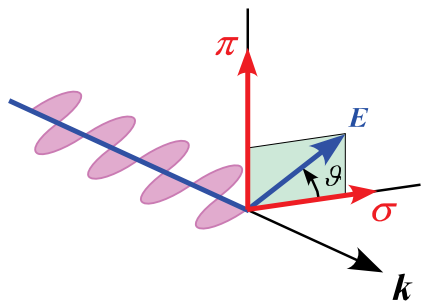
3. Expectations for the next generation light source

- Evaluation of L/S by NRXMS: Sr_2IrO_4
- Discrimination of spin chirality by NRXMS: DyMnO_3
- Improvement in the photon flux density

Matrix representation of polarization

Electric field

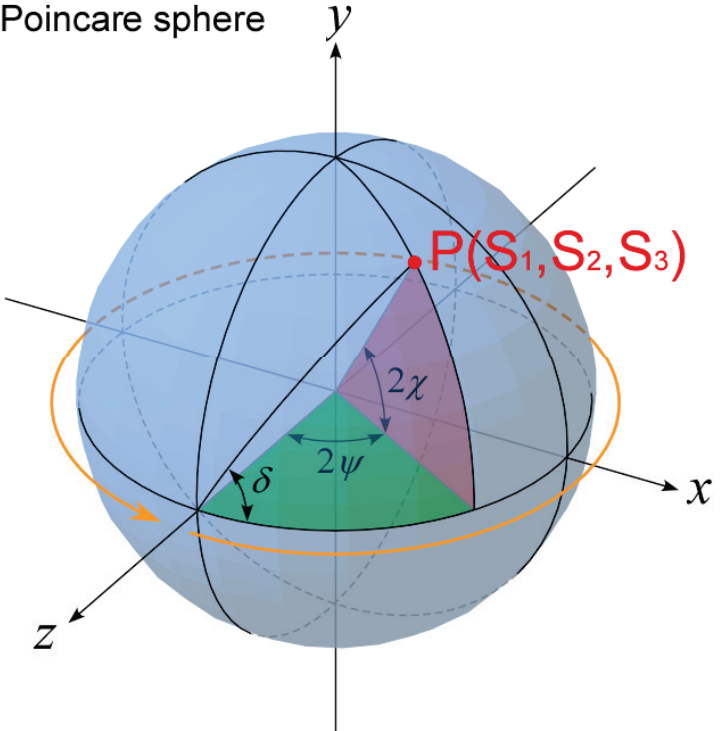
$$\mathbf{E}(\mathbf{r}, t) = \begin{pmatrix} E_\sigma e^{i\delta_\sigma} \\ E_\pi e^{i\delta_\pi} \end{pmatrix} e^{i(\omega t - \mathbf{k} \cdot \mathbf{r})}$$



Density matrix

$$\begin{aligned} \hat{\rho} &= \frac{\mathbf{E}(\mathbf{r}, t)\mathbf{E}^\dagger(\mathbf{r}, t)}{E_\sigma^2 + E_\pi^2} \\ &= \frac{1}{2} \left[\begin{pmatrix} 1 & 0 \\ 0 & 1 \end{pmatrix} + P_{45} \begin{pmatrix} 0 & 1 \\ 1 & 0 \end{pmatrix} + P_C \begin{pmatrix} 0 & -i \\ i & 0 \end{pmatrix} + P_L \begin{pmatrix} 1 & 0 \\ 0 & -1 \end{pmatrix} \right] \end{aligned}$$

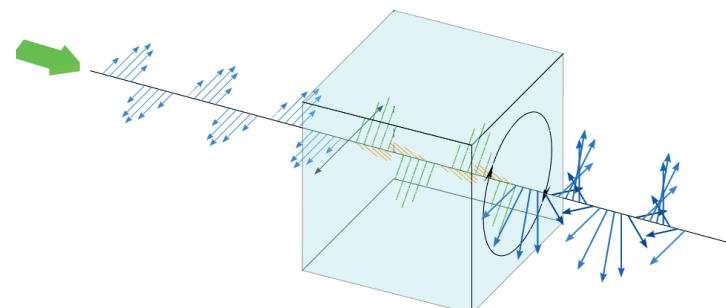
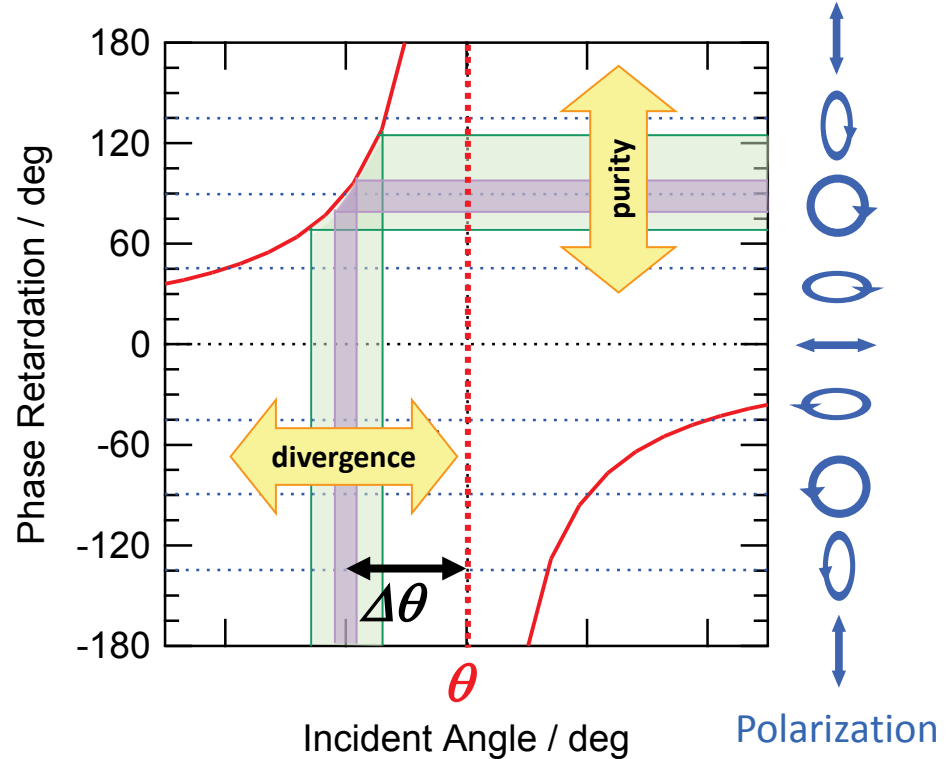
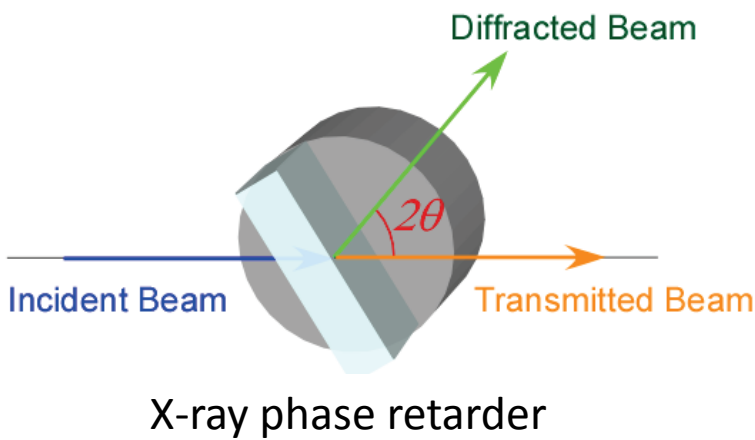
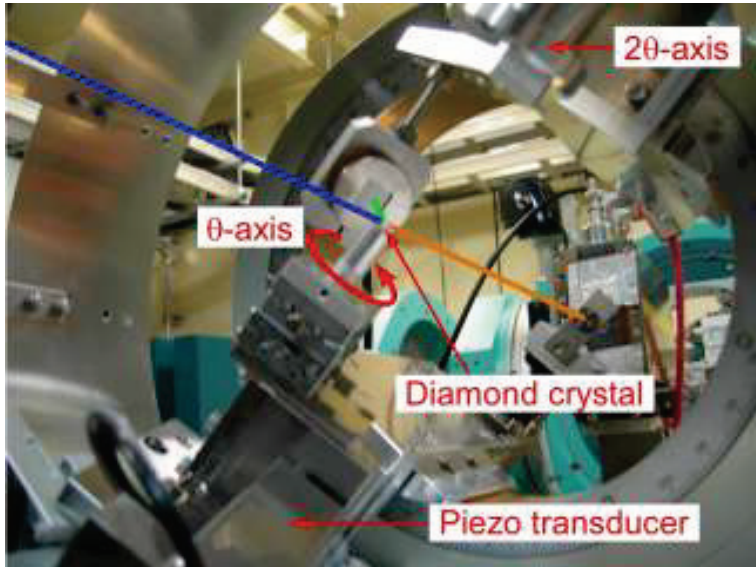
Poincare sphere



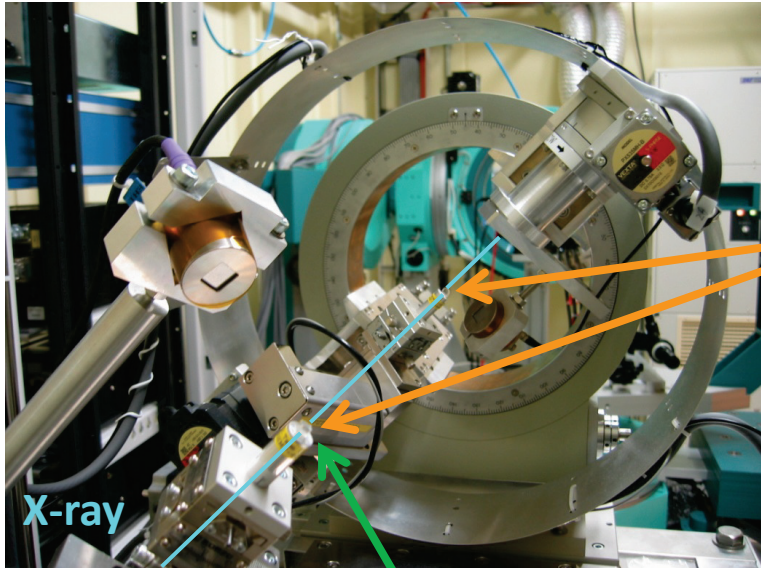
Stokes parameters

$$\mathbf{P} = (P_{45}, P_C, P_L) = \left(\frac{2E_\sigma E_\pi}{E_\sigma^2 + E_\pi^2} \cos(\delta_\sigma - \delta_\pi), -\frac{2E_\sigma E_\pi}{E_\sigma^2 + E_\pi^2} \sin(\delta_\sigma - \delta_\pi), \frac{E_\sigma^2 - E_\pi^2}{E_\sigma^2 + E_\pi^2} \right)$$

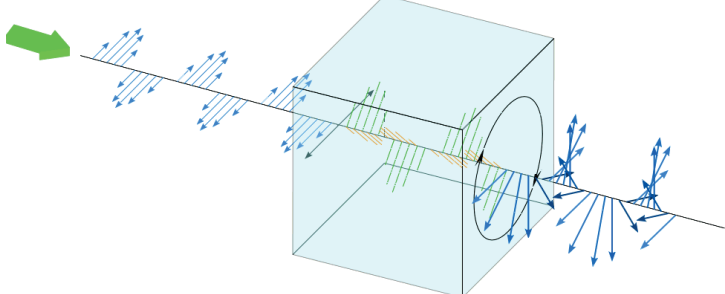
Manipulation of X-ray polarization



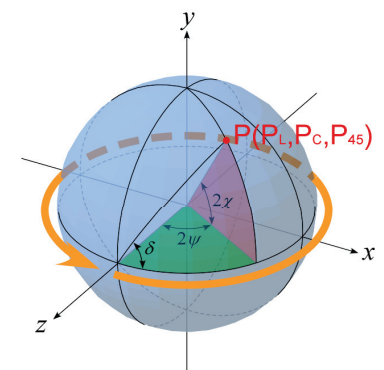
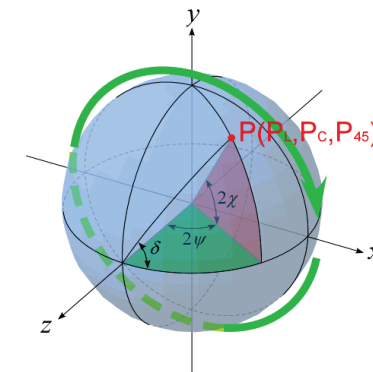
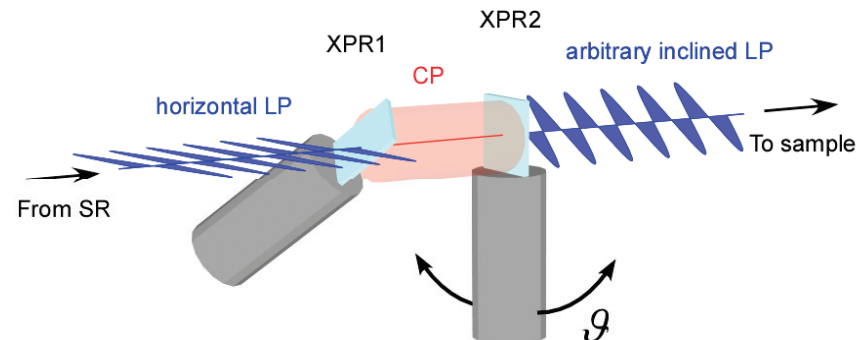
Manipulation of X-ray polarization



Elliptical polarization ($P_C^2 + P_L^2 = 1$)



Inclined linear polarization ($P_{45}^2 + P_L^2 = 1$)



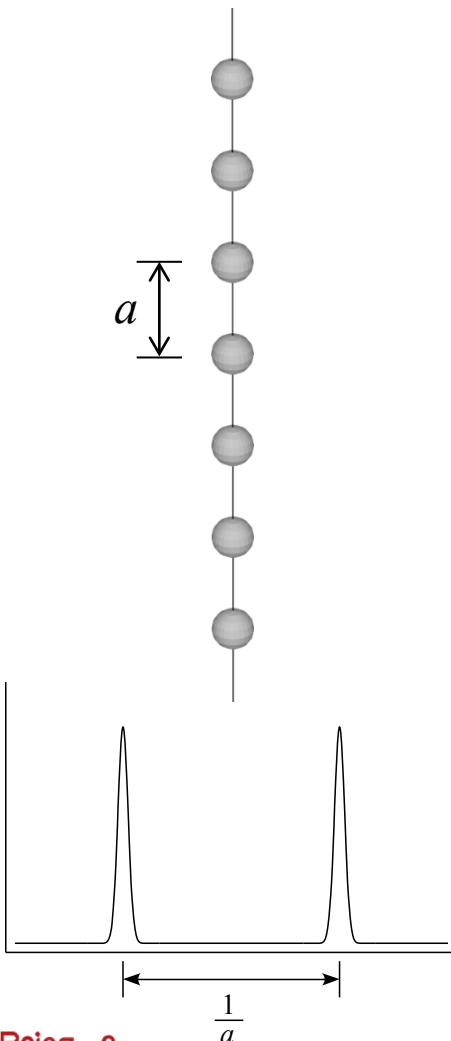
Transformation into arbitrary polarization

Outline

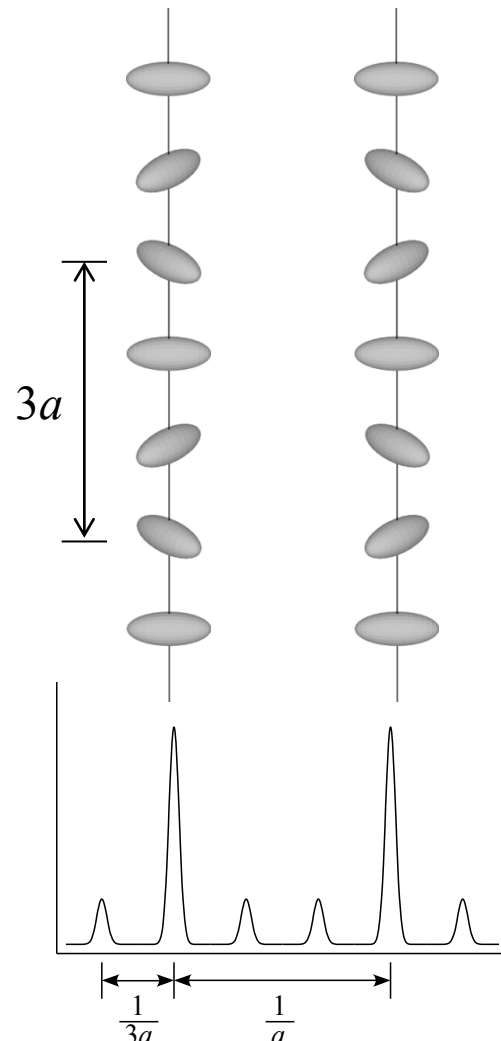
1. Microanalysis
 - X-ray focusing optics at BL19LXU/SPring-8
 - Operand XRD measurement on an EDLT device
2. Visualization of domain structures
 - Polarized X-ray diffractometry
 - **Chirality domain structure of CsCuCl_3**
 - Antiferromagnetic domain structure of $\text{Cd}_2\text{Os}_2\text{O}_7$
3. Expectations for the next generation light source
 - Evaluation of L/S by NRXMS: Sr_2IrO_4
 - Discrimination of spin chirality by NRXMS: DyMnO_3
 - Improvement in the photon flux density

Resonant circularly polarized X-Ray diffraction

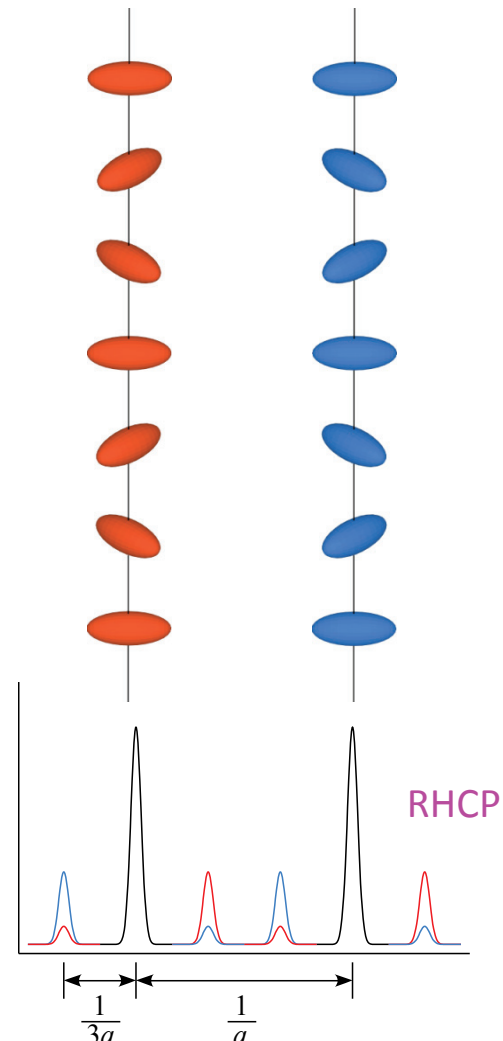
Non Resonant XRD



Resonant LP XRD

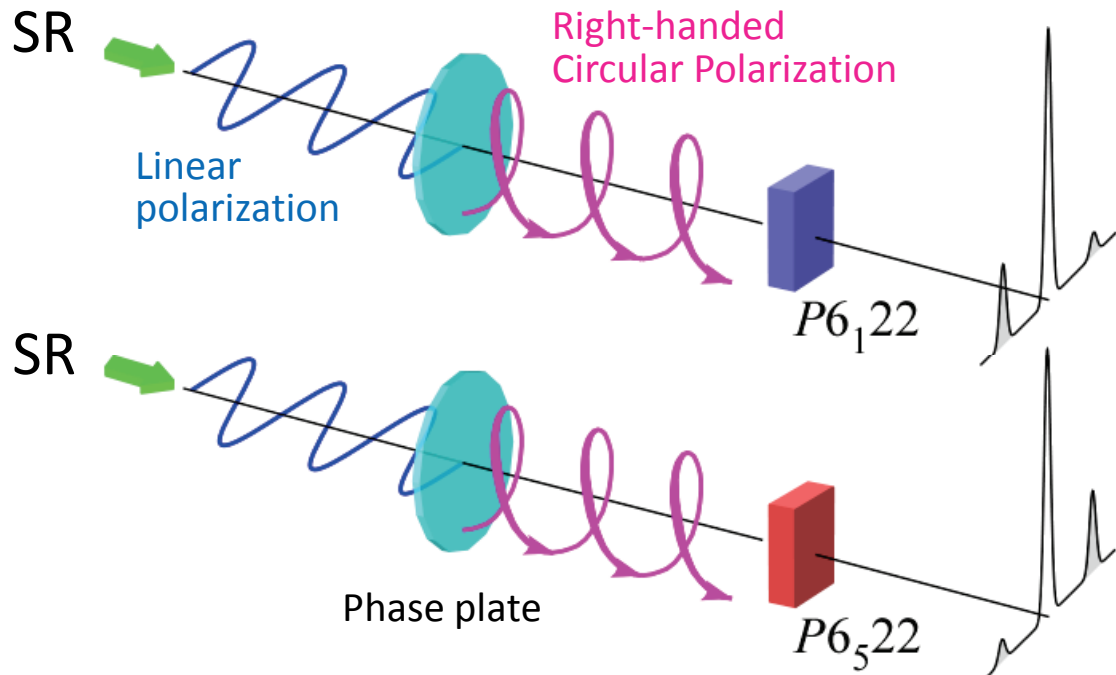


Resonant CP XRD

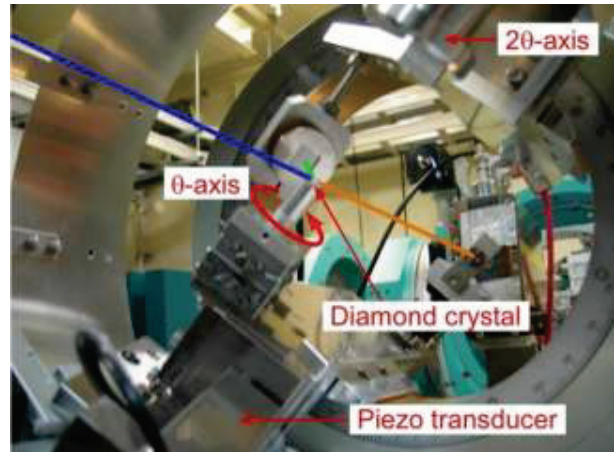


Experimental detail

Beamline: BL19LXU/SPring-8
X-ray energy: Cu K-edge
Phase Plate: C(001) t=1.0mm
X-ray detector: AMPTEK XR100-CR (Si-PIN)
Sample cooling: Closed-cycle He gas refrigerator



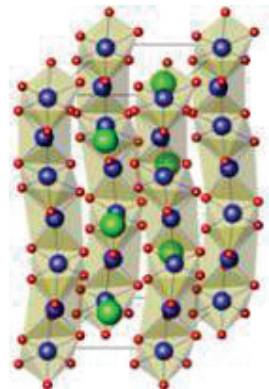
Six-circle diffractometer



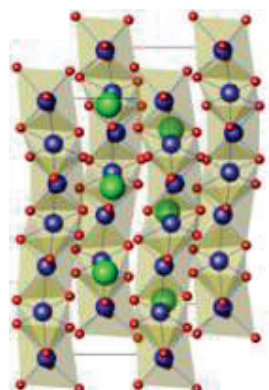
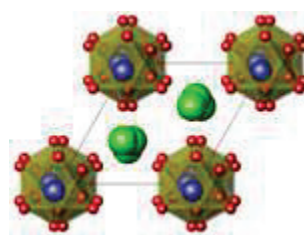
X-ray phase retarder

Discrimination of enantiomorph crystals

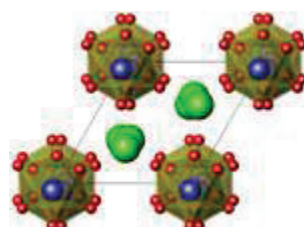
CsCuCl_3



Right-handed
 $P6_122$



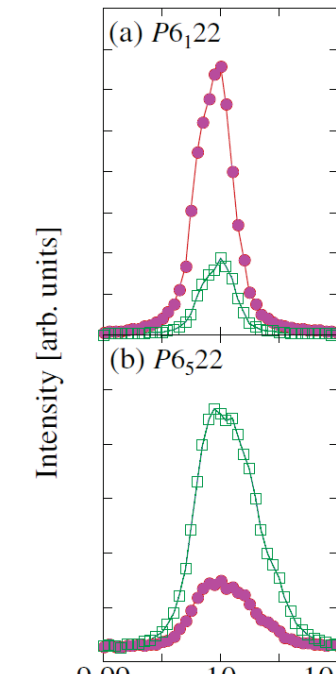
Left-handed
 $P6_522$



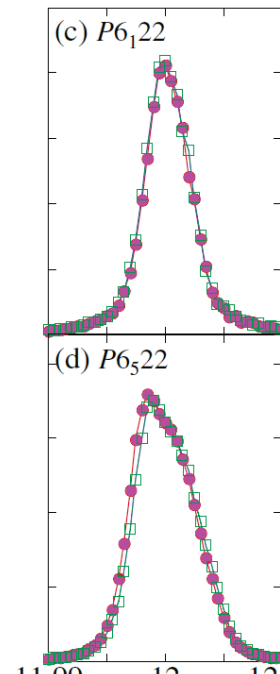
Asymmetrical superlattice reflection intensity



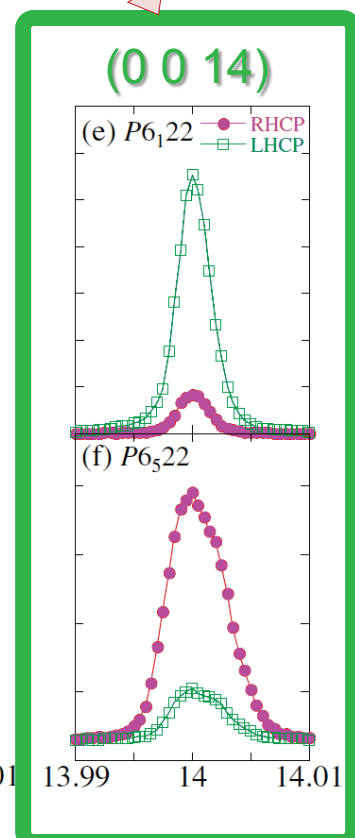
(0 0 10)



(0 0 12)

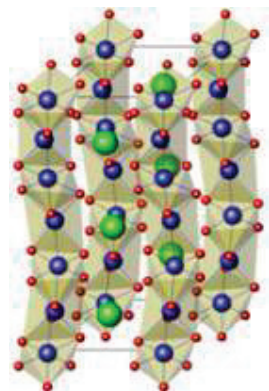


(0 0 14)

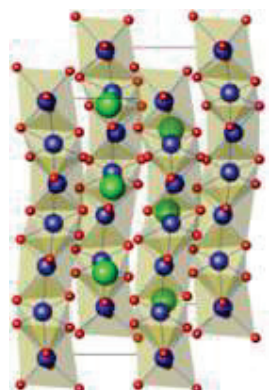
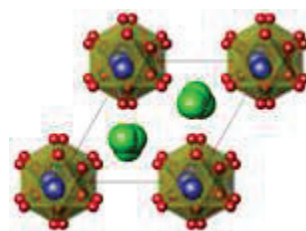


— RHCP
— LHCP

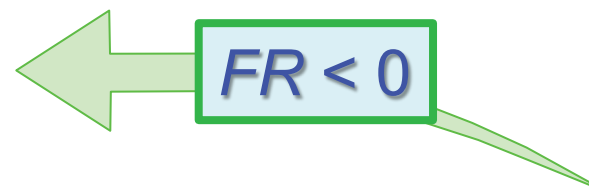
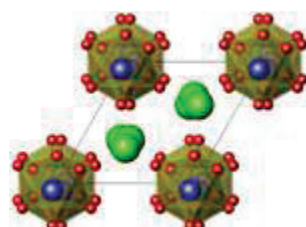
Flipping ratio (measure of handedness)



Right-handed
 $P_{6_1}22$

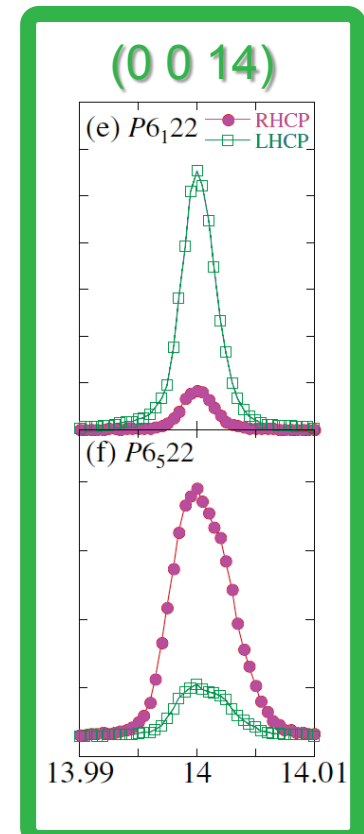
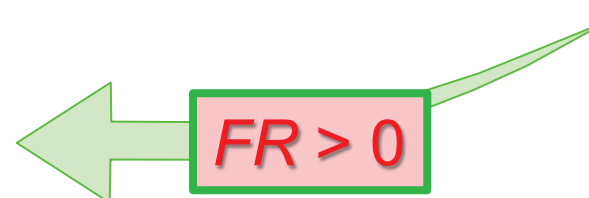


Left-handed
 $P_{6_5}22$

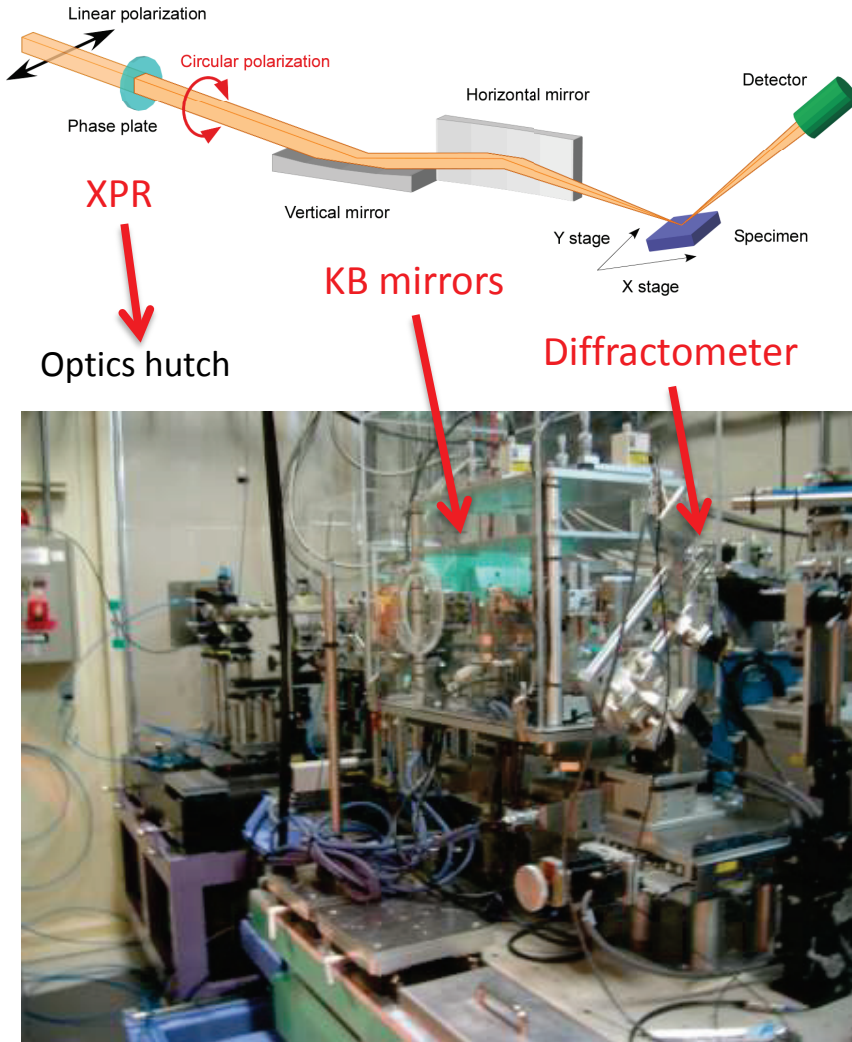


Flipping Ratio

$$FR = \frac{I(RHC) - I(LHC)}{I(RHC) + I(LHC)}$$

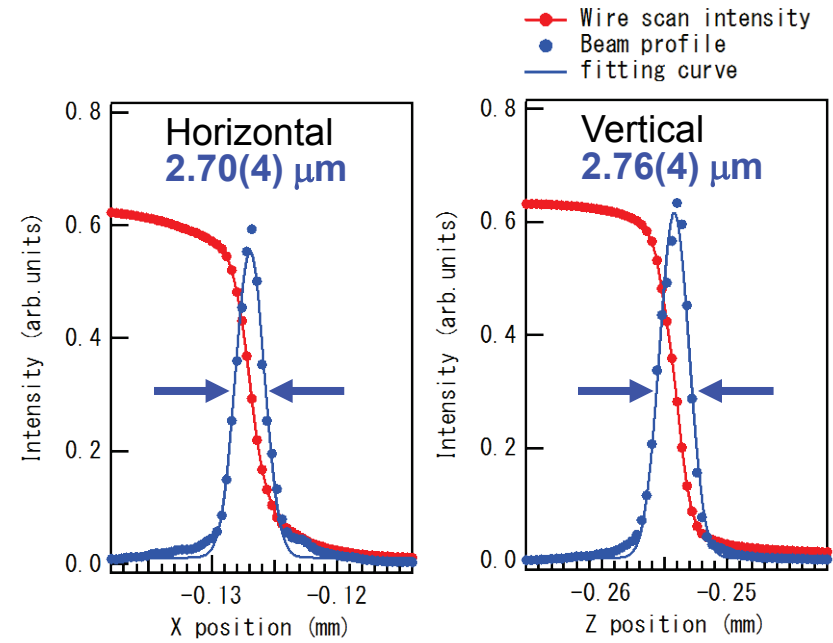


Experimental detail

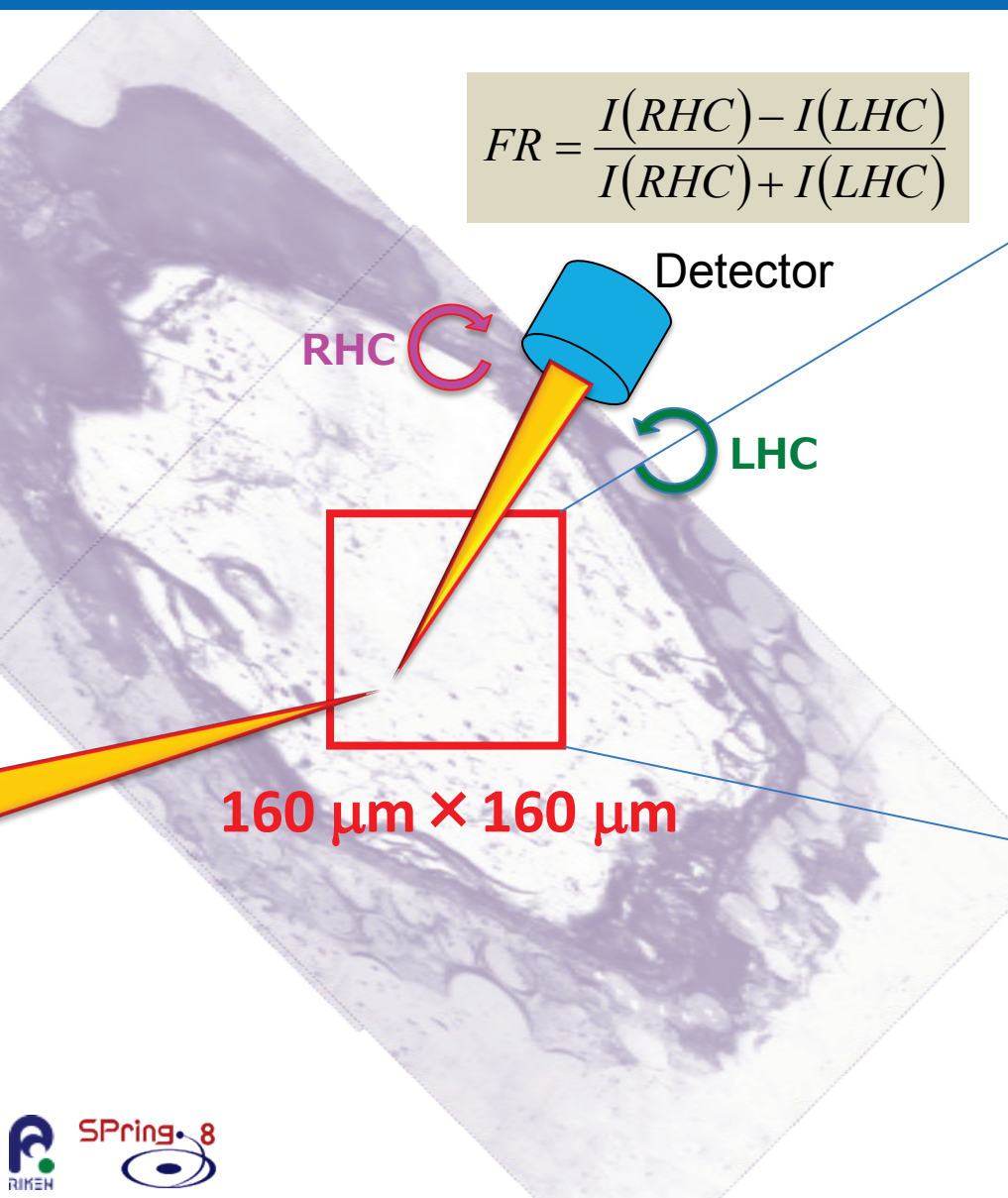


BL39XU/SPring-8

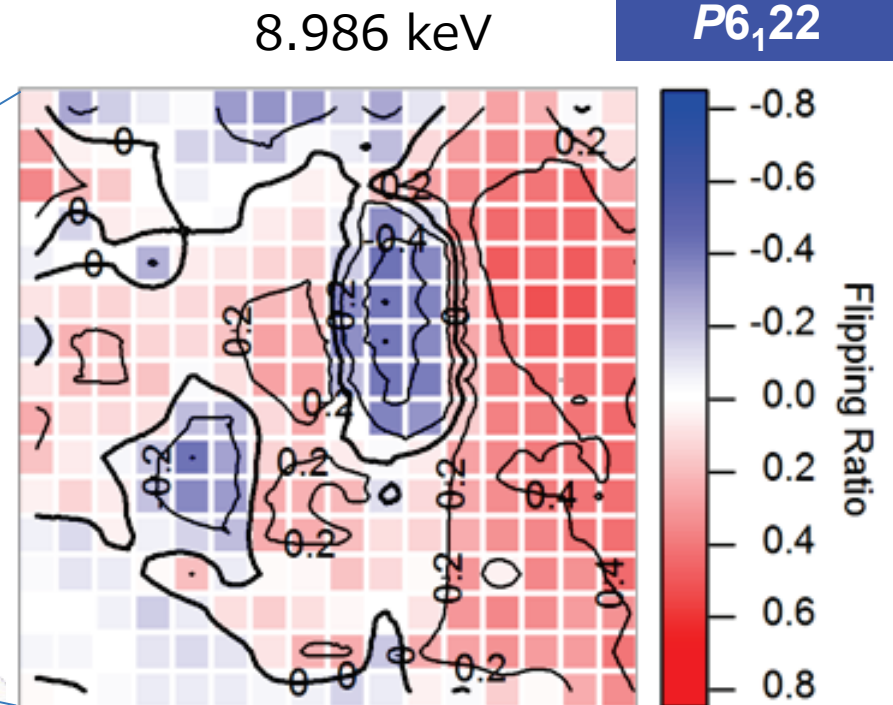
- X-ray (Cu K-edge)
- Detector (SDD)
- $P_c \approx \pm 0.993$ (simulation)
- Beam size @ sample position



Chirality domain structure on the (001) surface

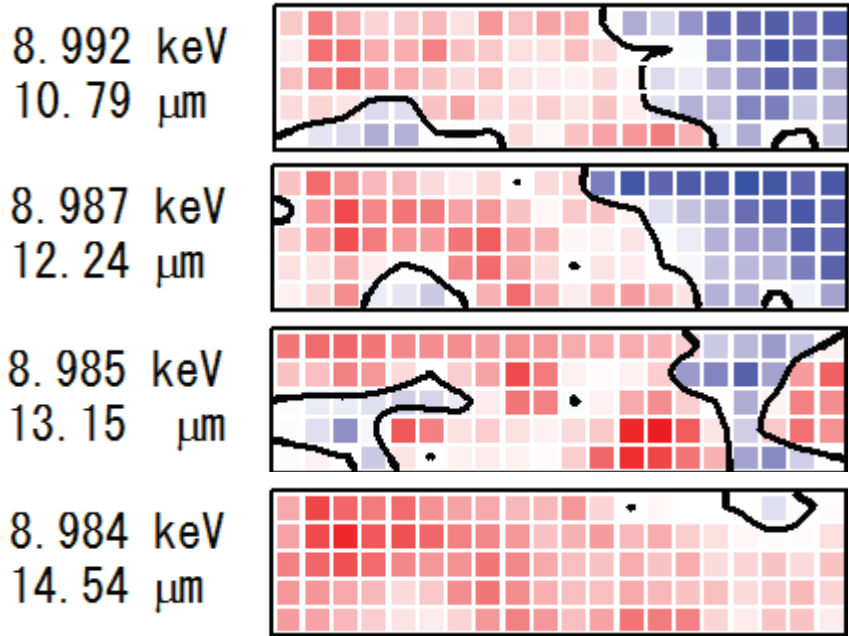
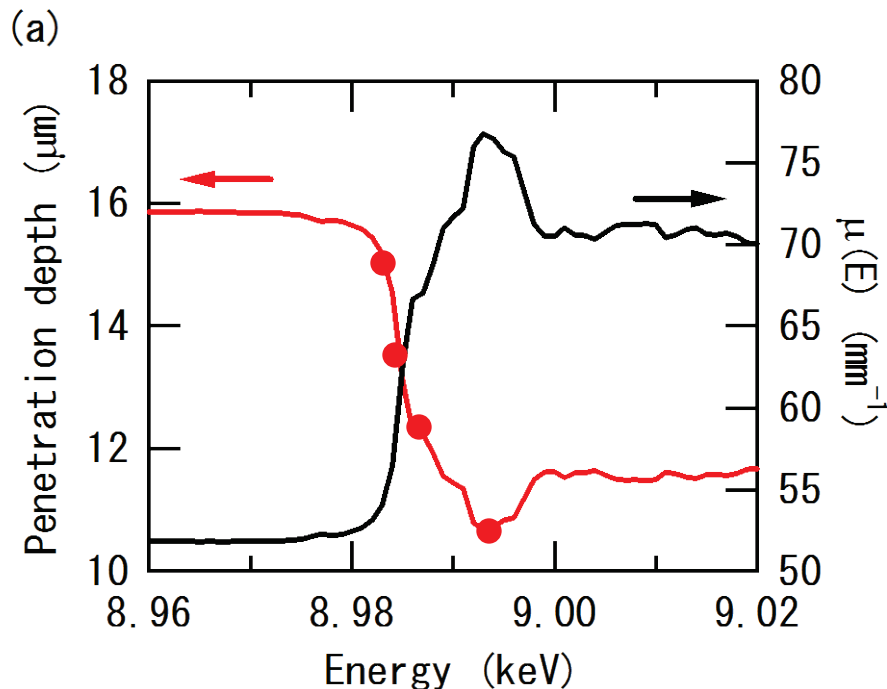


$$FR = \frac{I(RHC) - I(LHC)}{I(RHC) + I(LHC)}$$



Beamsize: $2.7 \times 2.7 \mu\text{m}^2$
Pitch: $10 \mu\text{m}$
Probing depth: $10.5 \mu\text{m}$

Depth profiling by controlling X-ray penetration

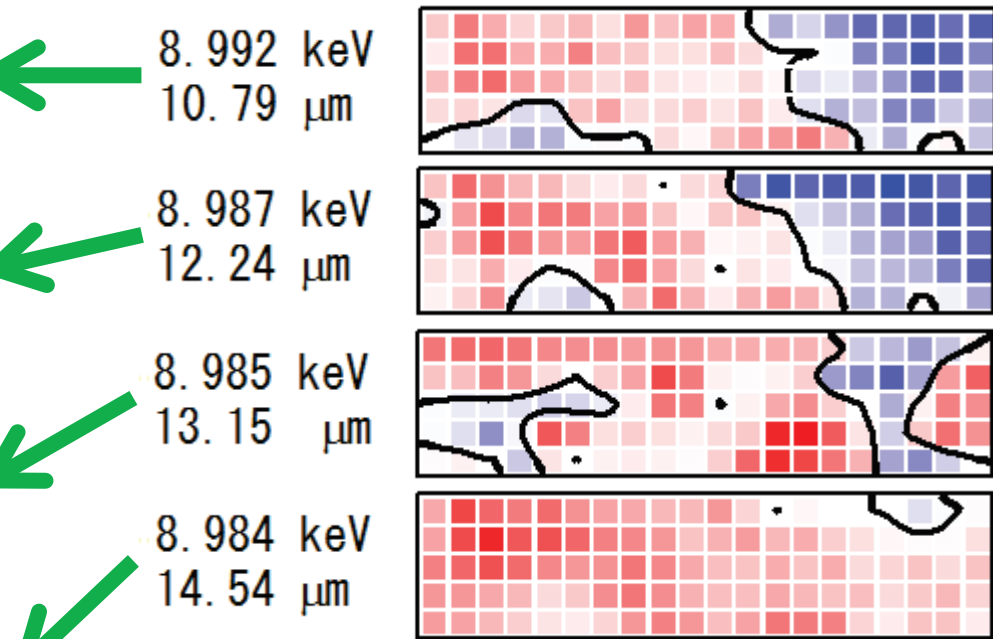
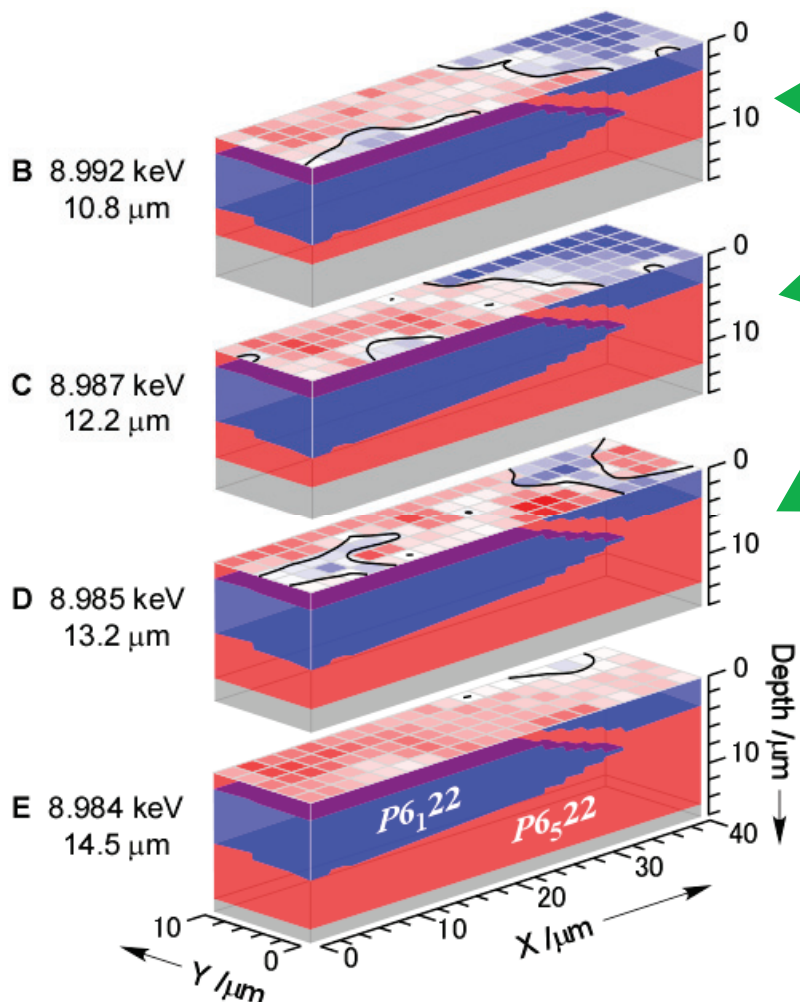


Observed Images depend on photon energy

Penetration depth depends on photon energy

Raster Image + Depth profile = 3D Image

3D imaging of chirality domain structure



Observed Images depend on photon energy

Morphological features

In-plane : several tens of microns

Out-of-plane : few microns

Outline

1. Microanalysis

- X-ray focusing optics at BL19LXU/SPring-8
- Operand XRD measurement on an EDLT device

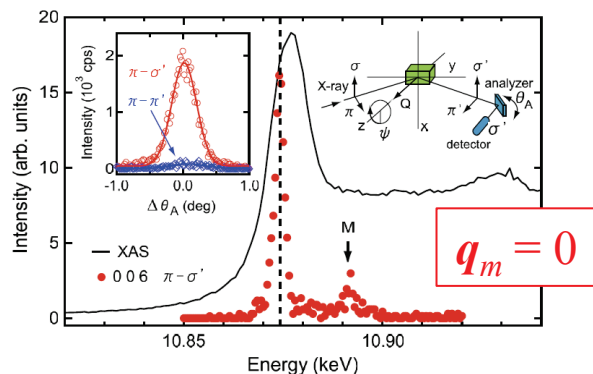
2. Visualization of domain structures

- Polarized X-ray diffractometry
- Chirality domain structure of CsCuCl_3
- **Antiferromagnetic domain structure of $\text{Cd}_2\text{Os}_2\text{O}_7$**

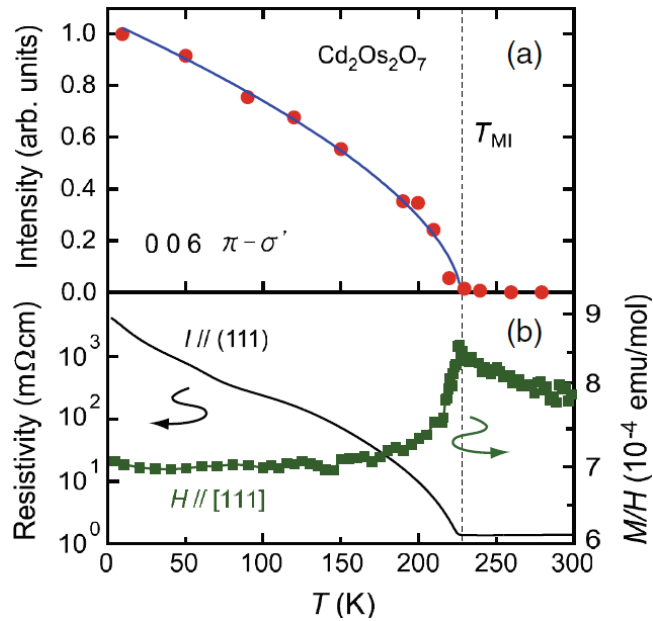
3. Expectations for the next generation light source

- Evaluation of L/S by NRXMS: Sr_2IrO_4
- Discrimination of spin chirality by NRXMS: DyMnO_3
- Improvement in the photon flux density

Determined magnetic structure of $\text{Cd}_2\text{Os}_2\text{O}_7$

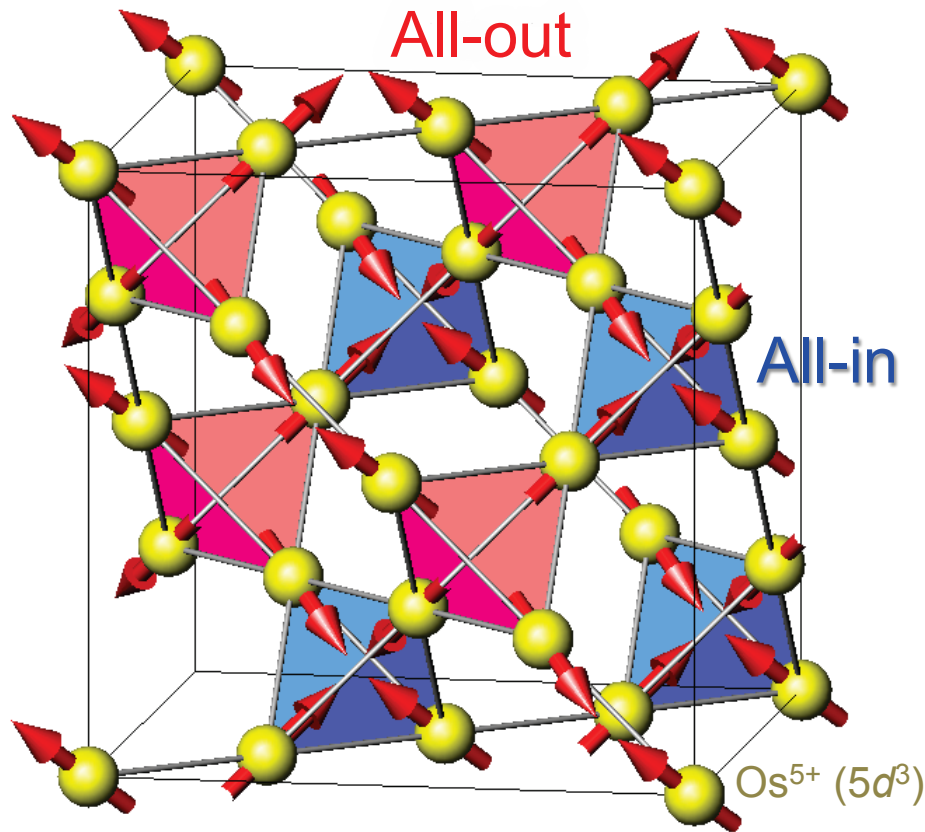


Spectra of the 006 reflection intensity



T dependence of the 006 reflection intensity

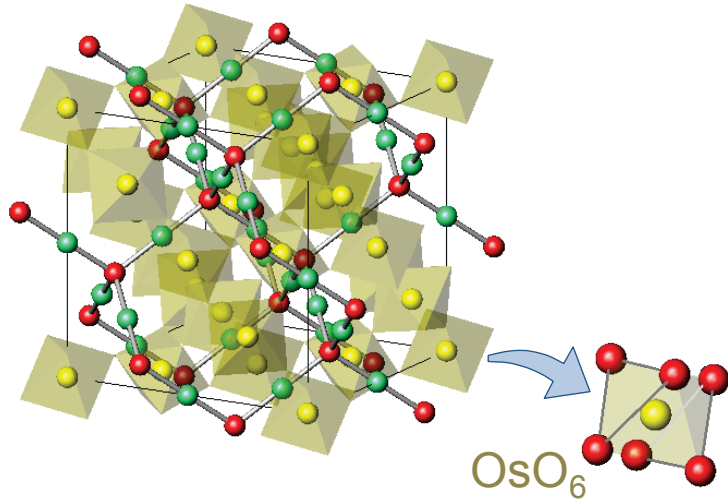
all-in-all-out type



Pyrochlore lattice of Os

Circularly polarized X-rays distinguish between AIAO and AOAI

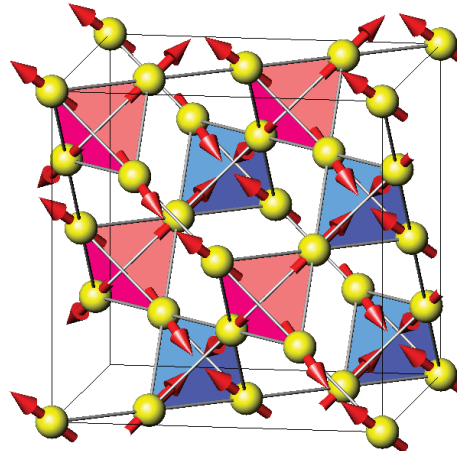
Anisotropy in Tensor Susceptibility



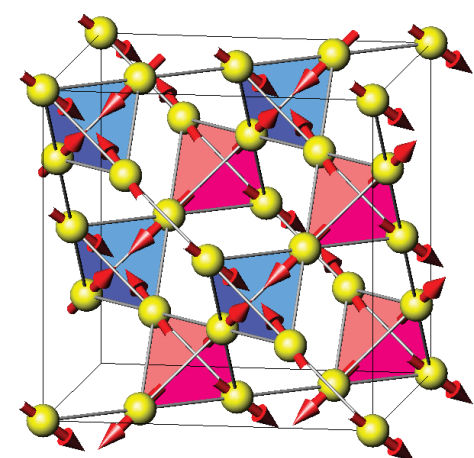
$$F_{\text{ATS}} \begin{pmatrix} \sin 2\Psi & -\sin \theta \cos 2\Psi \\ \sin \theta \cos 2\Psi & \sin^2 \theta \sin 2\Psi \end{pmatrix}$$

$$I_{004n+2}(P_C) \propto |F_{\text{ATS}}|^2 [\sin^2 \theta + 2 \sin^2 \Psi \cos^2 \Psi \cos^4 \theta] + |F_{\text{mag}}|^2 \sin^2 \theta \boxed{\mp} \boxed{P_C} \text{Re}[F_{\text{ATS}}^* F_{\text{mag}}] \sin 2\Psi \sin \theta \cos^2 \theta$$

All-In/All-Out



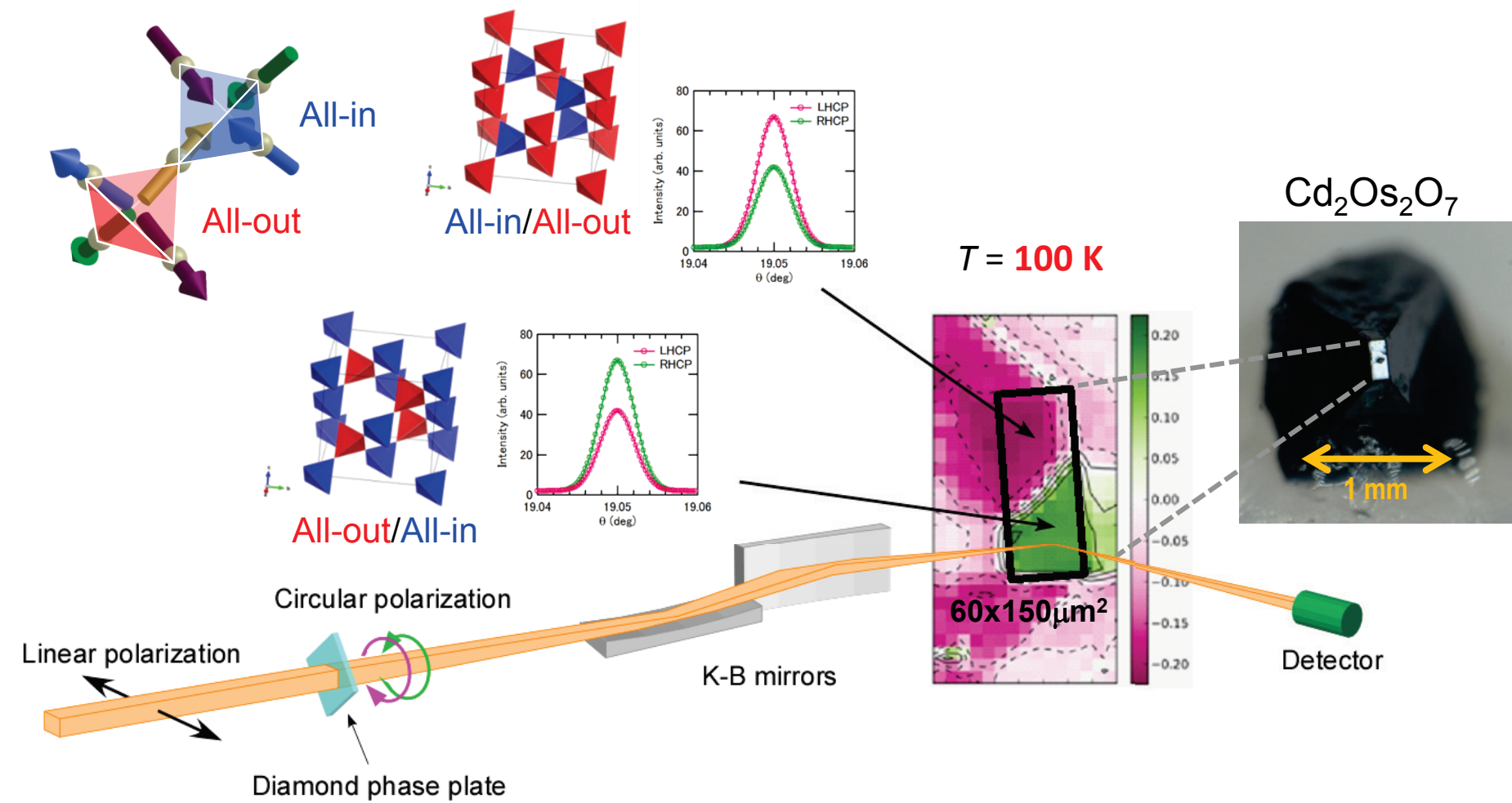
All-Out/All-In



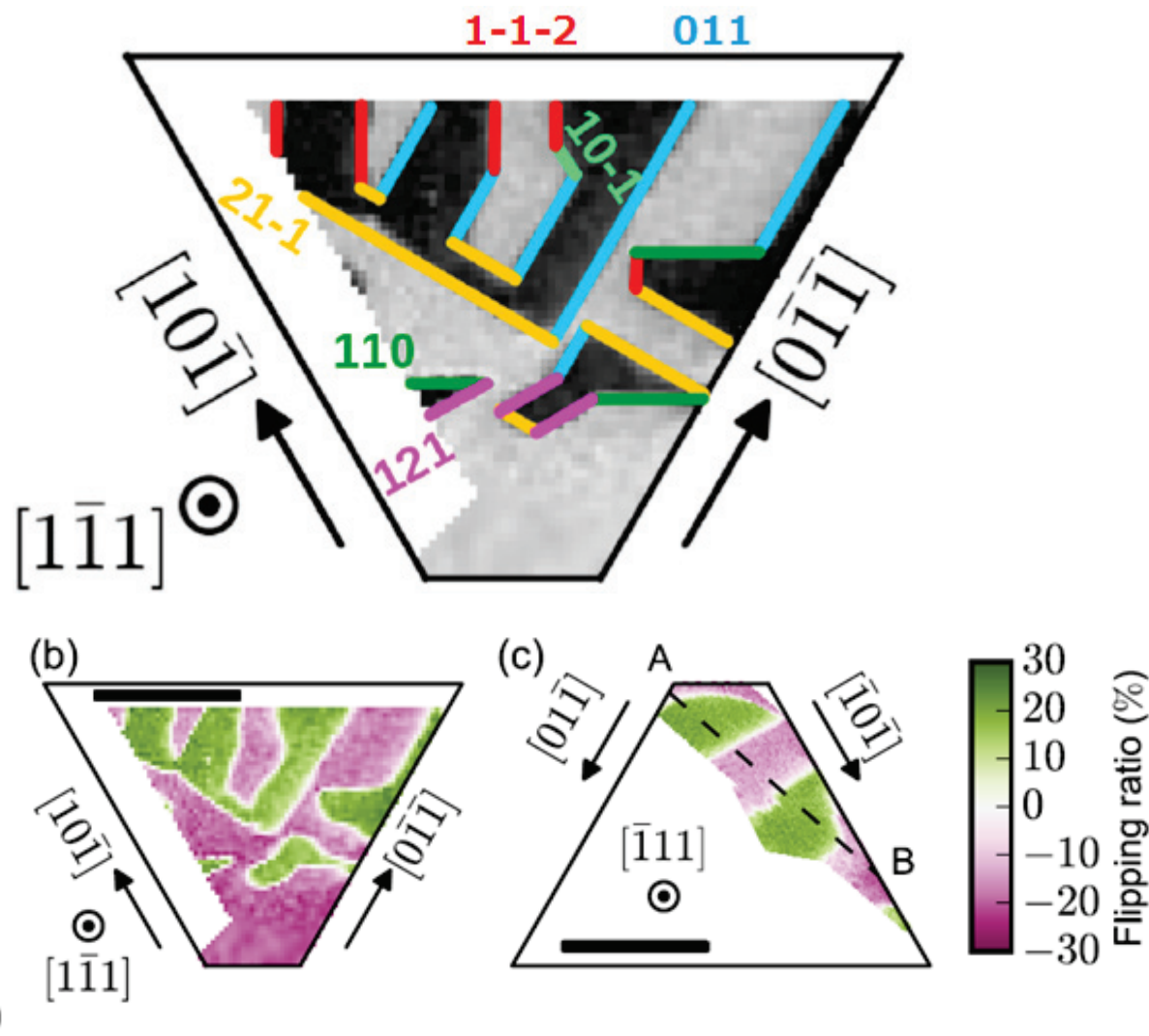
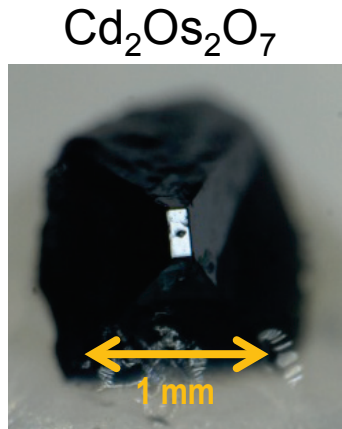
$$F_{\text{mag}} \begin{pmatrix} 0 & i \sin \theta \\ i \sin \theta & 0 \end{pmatrix} \quad - F_{\text{mag}} \begin{pmatrix} 0 & i \sin \theta \\ i \sin \theta & 0 \end{pmatrix}$$

$P_c = +1$: RHC
 $P_c = -1$: LHC

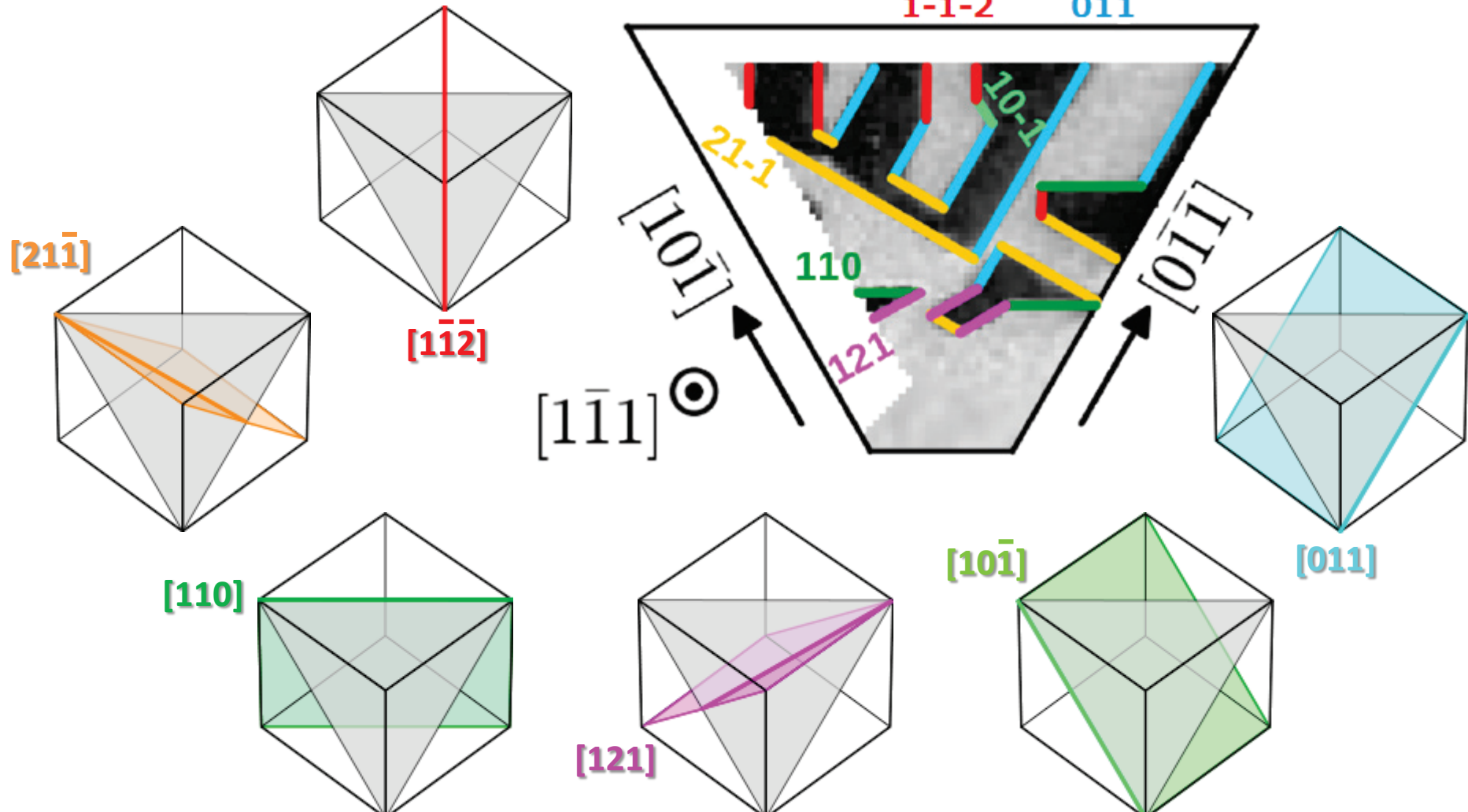
Magnetic domain structure on the (001) surface



Magnetic domain structure on the other facets



Identification of magnetic domain walls



Outline

1. Microanalysis

- X-ray focusing optics at BL19LXU/SPring-8
- Operand XRD measurement on an EDLT device

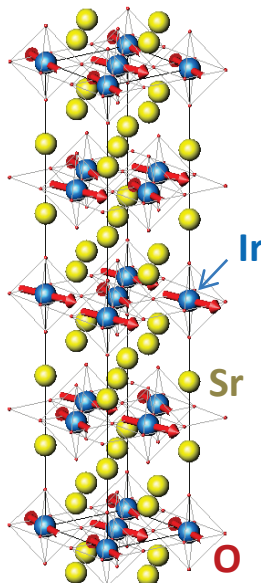
2. Visualization of domain structures

- Polarized X-ray diffractometry
- Chirality domain structure of CsCuCl_3
- Antiferromagnetic domain structure of $\text{Cd}_2\text{Os}_2\text{O}_7$

3. Expectations for the next generation light source

- Evaluation of L/S by NRXMS: Sr_2IrO_4
- Discrimination of spin chirality by NRXMS: DyMnO_3
- Improvement in the photon flux density

Relativistic Mott insulator Sr_2IrO_4

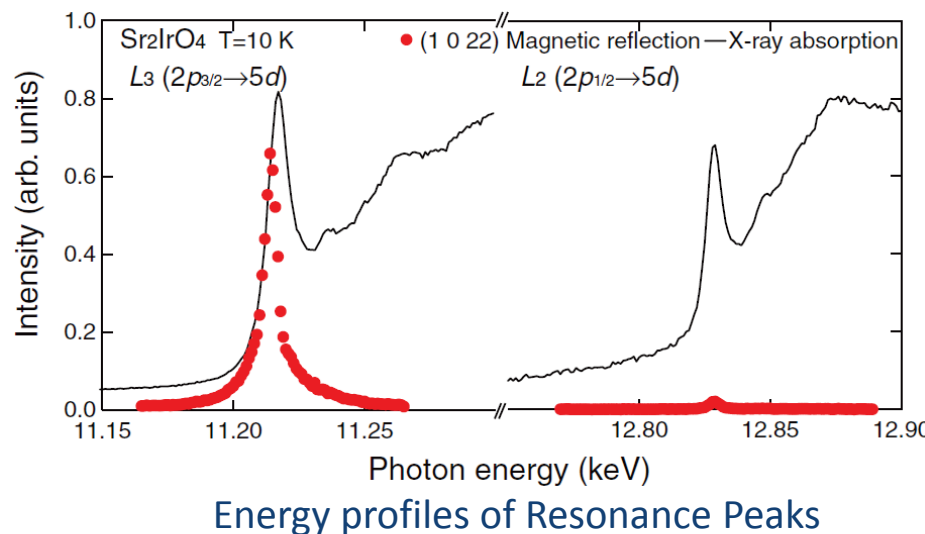


Magnetic structure

$\text{Ir}^{4+} (5d^5)$

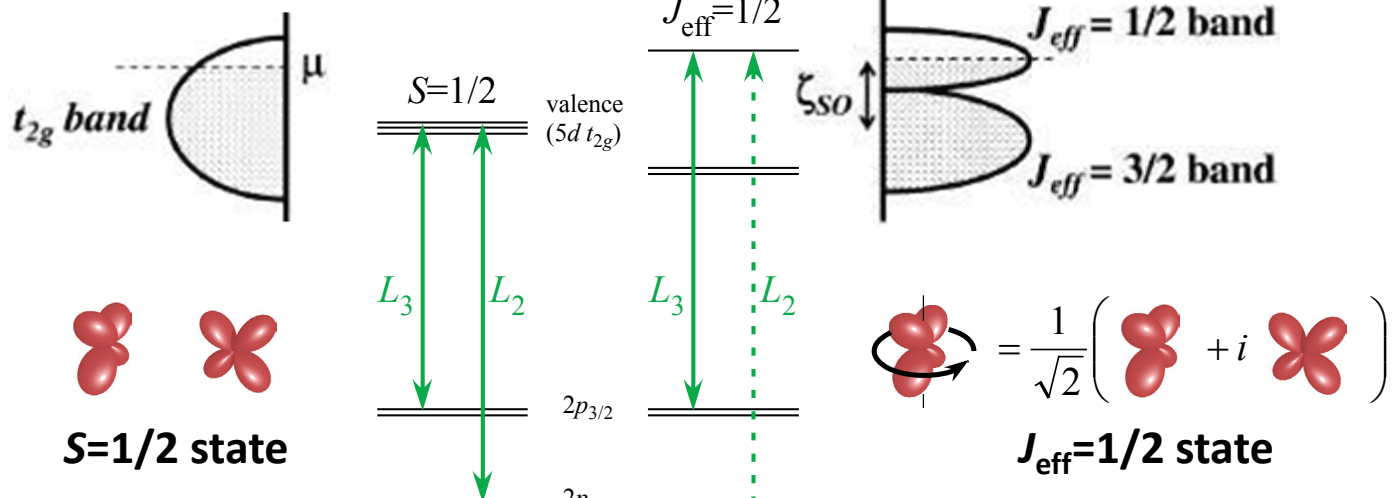
$\mu_{\text{eff}} \sim 0.5 \mu_B$

Insulator

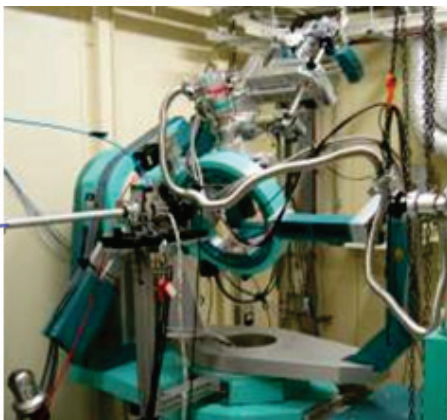
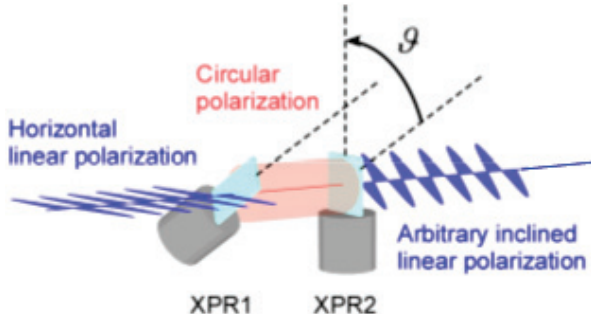


$S=1/6, L=2/3$

$\mu_{\text{eff}} = 0.77 \mu_B$



Evaluation of L/S by non-resonant X-ray magnetic scattering



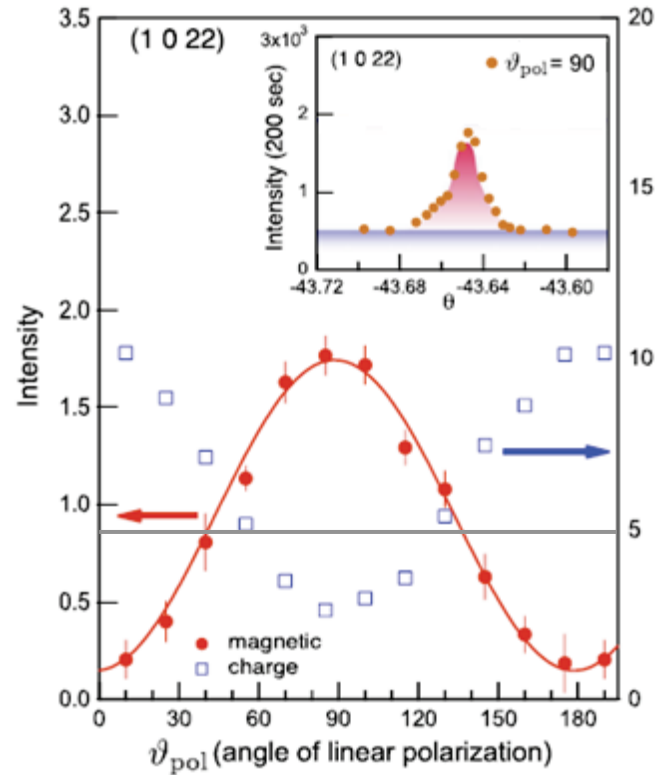
$$I(\vartheta) = I_0 + I_{45} \sin 2\vartheta + I_L \cos 2\vartheta$$

Charge

$$\begin{cases} I_0 = |F(K)|^2 (\sin^4 \theta + \cos^4 \theta) \\ I_{45} = 0, \quad I_L = |F(K)|^2 2 \sin^2 \theta \cos^2 \theta \end{cases}$$

Magnetic

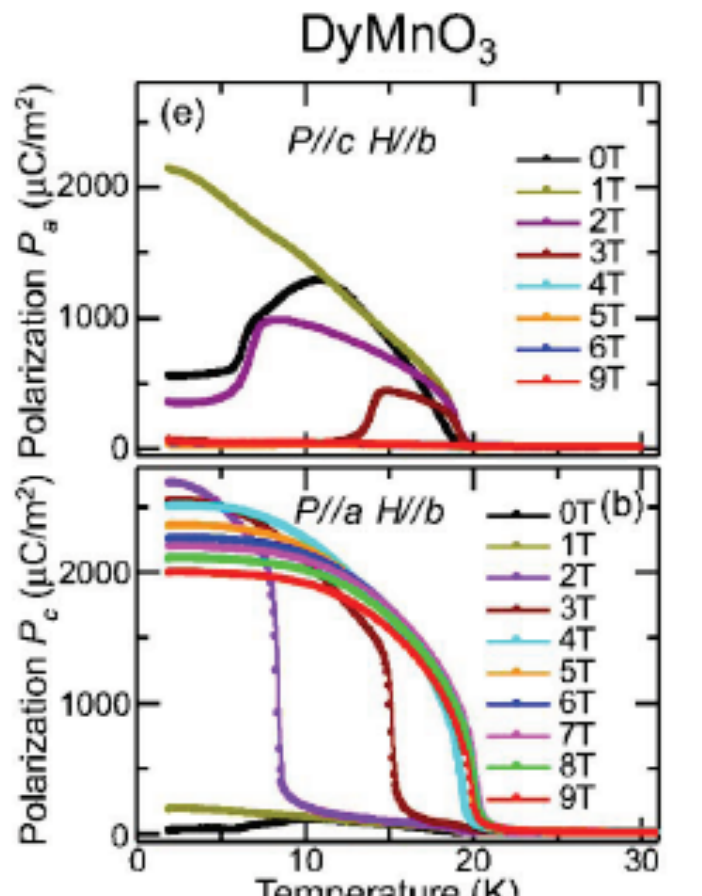
$$\begin{cases} I_0 = \left(\frac{\hbar \omega}{mc^2} \sin \theta \sin 2\theta \right)^2 |S(K)|^2 \left[\left(\frac{1}{\sin \theta} + \frac{2L \sin \theta}{S} \right)^2 - \left(\frac{2L \sin \theta}{S} \right) \left(\frac{1}{\sin \theta} + \frac{L \sin \theta}{S} \right) \right] \\ I_{45} = 0, \quad I_L = - \left(\frac{\hbar \omega}{mc^2} \sin \theta \sin 2\theta \right)^2 |S(K)|^2 \left[\left(\frac{2L \sin \theta}{S} \right) \left(\frac{1}{\sin \theta} + \frac{L \sin \theta}{S} \right) \right] \end{cases}$$



$$J_{eff} = \frac{1}{2}, \quad \frac{L}{S} = 5.0 \pm 0.7$$

$$S = \frac{1}{2}, \quad \frac{L}{S} = 0$$

Multiferroic material DyMnO_3

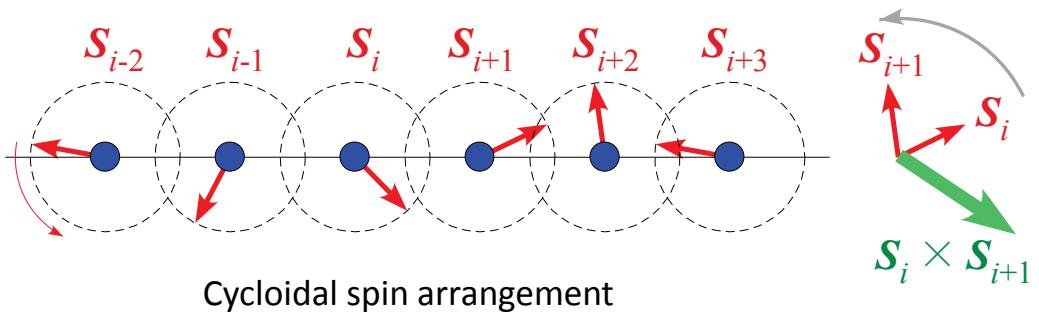


Temperature dependence of polarization.

T. Kimura et al., PRB **71**, 224425 (2005).

Spin-chirality driven ferroelectrics

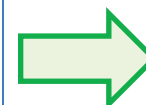
Magnetic structure having **vector spin chirality**



Cycloidal spin arrangement

Spontaneous activation of Dzyaloshinskii-Moriya interaction $\mathcal{H}_{DM} = \mathbf{D} \cdot (\mathbf{S}_1 \times \mathbf{S}_2)$ in order to reduce total energy.

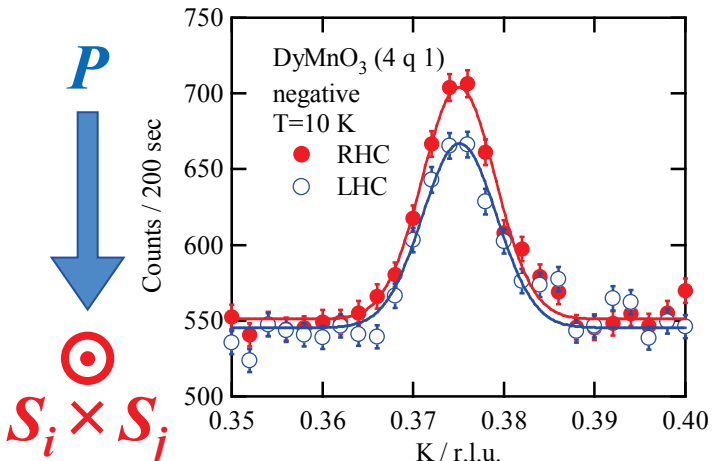
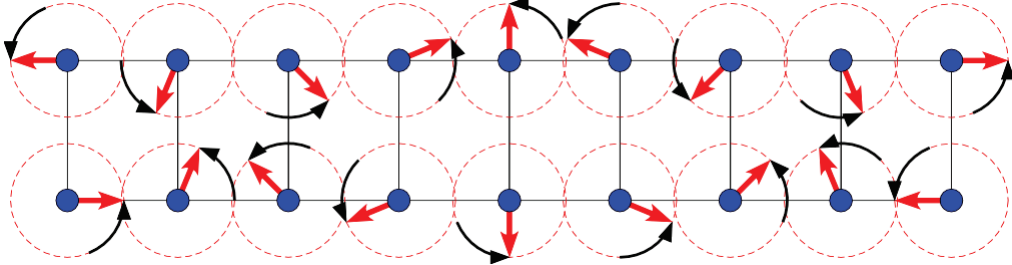
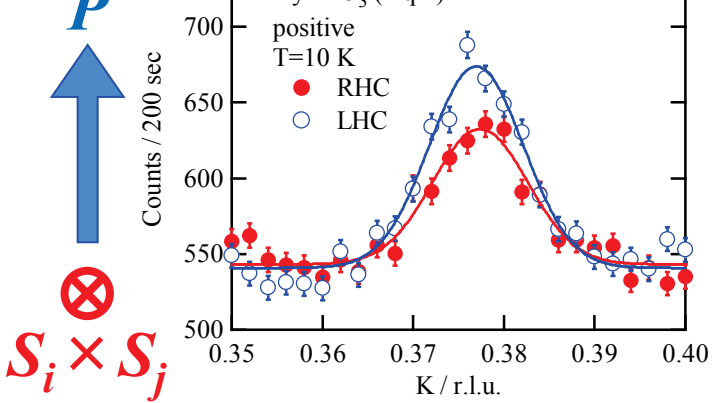
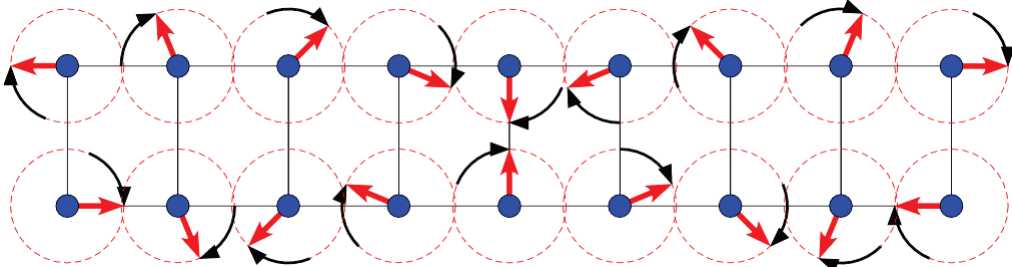
$\mathbf{D} = 0$
centrosymmetric
non-polar



$\mathbf{D} \neq 0$
non-centrosymmetric
local polarization

Violation of inversion symmetry

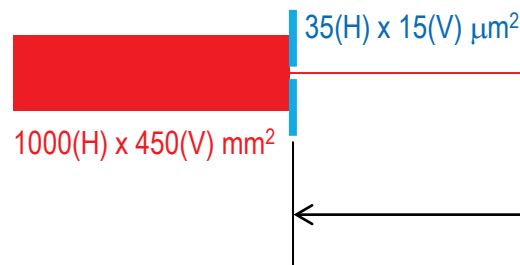
Discrimination of vector spin chirality by NRXMS



The flux density will increase three orders of magnitude

BL19LXU/SPring-8

Secondary Light Source
64 m from ID



70000 mm

Focal Point
100(H) x 100(V) nm^2
 3.7×10^{10} photons/s

Focusing Mirrors

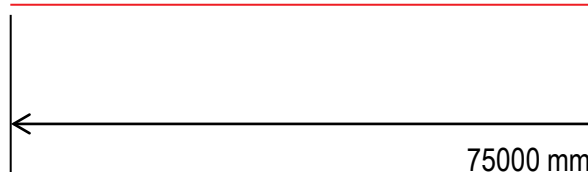
260 mm

200 mm

SPring-8-II (Conceptual Design Report)

Light Source

56.5(H) x 13.2(V) mm^2



Focusing Mirrors

450 mm

300 mm

Focal Point
230(H) x 150(V) nm^2
 5.0×10^{13} photons/s

Future prospects

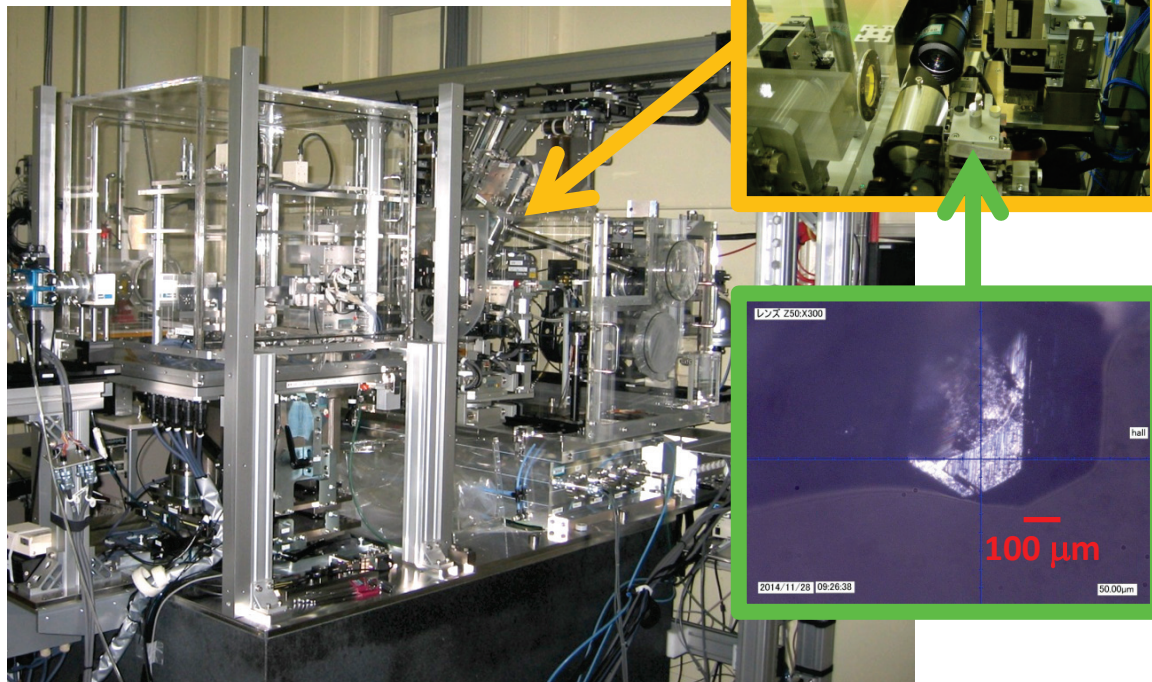
Polarized nanobeam X-ray diffraction techniques offer new opportunities to investigate hierarchical structures in real materials.

One of the most promising applications is the visualization of spatial variation of order parameters.

A thousand times more intense X-ray nanobeam allows the visualization of order parameters using NRXMS.

High-resolution scanning X-ray microscope

BL19LXU/SPring-8



KB mirror optics and diffractometer

3.7×10^{10} photons/s @ $100 \times 100 \text{ nm}^2$

For LT experiments

He flow



N₂ flow



Sample

